Provided for non-commercial research and education use.
Not for reproduction, distribution or commercial use.

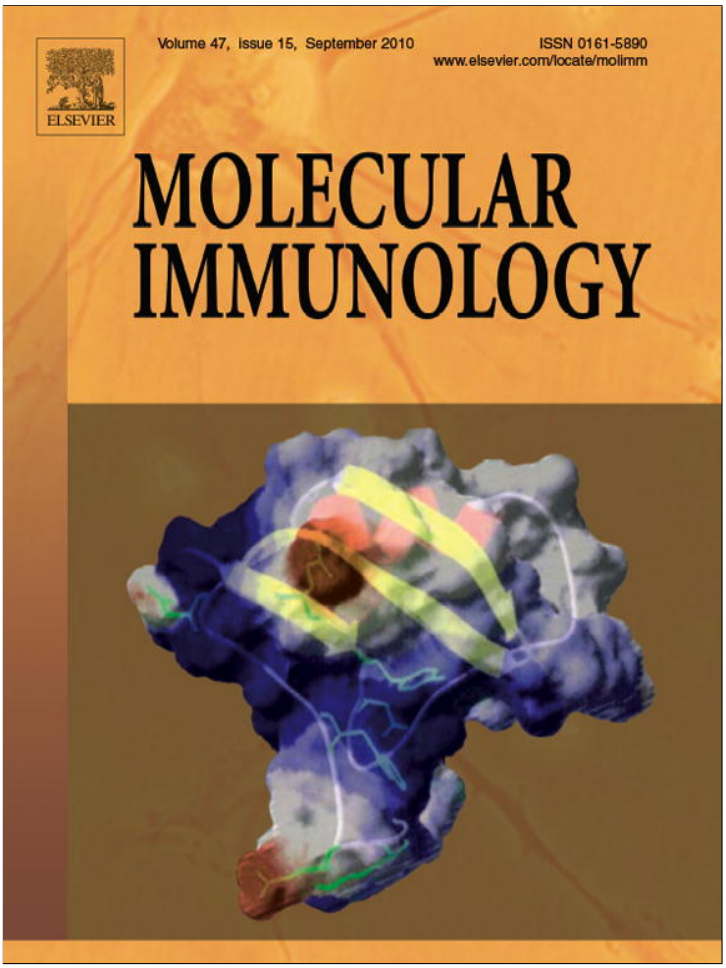

This article appeared in a journal published by Elsevier. The attached copy is furnished to the author for internal non-commercial research and education use, including for instruction at the authors institution and sharing with colleagues.

Other uses, including reproduction and distribution, or selling or licensing copies, or posting to personal, institutional or third party websites are prohibited.

In most cases authors are permitted to post their version of the article (e.g. in Word or Tex form) to their personal website or institutional repository. Authors requiring further information regarding Elsevier's archiving and manuscript policies are encouraged to visit:

http://www.elsevier.com/copyright

Author's personal copy

Molecular Immunology 47 (2010) 2492–2504

Contents lists available at ScienceDirect

Molecular Immunology

journal homepage: www.elsevier.com/locate/molimm

Human perforin permeabilizing activity, but not binding to lipid membranes, is affected by pH

Tilen Praper[a,2], Mojca Podlesnik Beseničar[a,1,2], Helena Istinič[a], Zdravko Podlesek[a], Sunil S. Metkar[b], Christopher J. Froelich[b], Gregor Anderluh[a,*]

[a] Department of Biology, Biotechnical Faculty, University of Ljubljana, Večna pot 111, 1000 Ljubljana, Slovenia
[b] Department of Medicine, NorthShore University Health Systems Research Institute, Evanston, IL, 60202, USA

ARTICLE INFO

Article history:
Received 10 May 2010
Received in revised form 31 May 2010
Accepted 2 June 2010
Available online 26 June 2010

Keywords:
Perforin
MACPF domain
Pore forming proteins
pH-dependence
Surface plasmon resonance

ABSTRACT

The various steps that perforin (PFN), a critical mediator of innate immune response, undertakes to form a transmembrane pore remains poorly understood. We have used surface plasmon resonance (SPR) to dissect mechanism of pore formation. The membrane association of PFN was calcium dependent irrespective of pH. However, PFN does not permeabilize large or giant unilamellar vesicles (GUV) at pH 5.5 even though the monomers bind to the membranes in the presence of calcium. It was possible to activate adsorbed PFN and to induce membrane permeabilization by simply raising pH to a physiological level (pH 7.4). These results were independently confirmed on GUV and Jurkat cells. The conformational state of PFN at either pH was further assessed with monoclonal antibodies Pf-80 and Pf-344. Pf-344 maps to a linear epitope within region 373–388 of epidermal growth factor (EGF)-like domain while the Pf-80 appears to recognize a conformational epitope. Pf-344 interacts with the EGF-like domain after PFN monomers undergo pore formation, the site recognized by Pf-80 is only accessible at acidic but not neutral pH. Thus, the Pf-80 mAb likely interacts with a region of the monomer that participates in oligomerization prior to insertion of the monomer into the lipid bilayer and thus may have therapeutic utility against PFN-mediated immunopathology.

© 2010 Elsevier Ltd. All rights reserved.

1. Introduction

Virus-infected or transformed cells are efficiently killed by cytotoxic T lymphocytes (CTL) and natural killer (NK) cells through the granule exocytosis and death receptor pathways (Voskoboinik et al., 2006). Perforin (PFN), a component of cytolytic granules, is essential for initiating apoptosis by bringing granzyme into the cytosol of the target cell. Two models predominate to explain PFN-dependent granzyme delivery. The granzymes may pass through transient pores formed in plasma membrane or, after endocytosis with granzymes, PFN facilitates their release in the cytosol (Voskoboinik et al., 2006; Pipkin and Lieberman, 2007). Despite the controversies, PFN is designed to deliver the granzymes *in vivo* and its destabilizing activity at cellular membranes appears to be a critical prerequisite.

Although much is known about the molecular events that lead to cell death after PFN-mediated granzyme delivery, the mechanism underlying transmembrane pore formation and biochemical properties that allow these pores to facilitate granzyme delivery remain elusive (Pipkin and Lieberman, 2007). The primary obstacle to understanding the biology of PFN has been the limited availability of native protein and the difficulties in expressing mature PFN monomers. A reliable recombinant expression system was developed only recently (Sutton et al., 2008).

PFN is a multidomain protein divisible into the membrane attack complex/perforin (MACPF) domain at the N-terminus, an EGF-like domain of unknown function, and a C2 domain at the C-terminus (Fig. 1A). The structure of MACPF domain is strikingly similar to domains 1–3 of cholesterol dependent cytolysins (CDC), pore forming toxins from Gram-positive bacteria (Rosado et al., 2008). Domain 3 of CDC contains two pairs of α-helices that upon membrane binding and oligomerization to a prepore complex then refolds into transmembrane β-hairpins that traverse the membrane to form the lining of a barrel-stave pore (Tweten, 2005). The

Abbreviations: AD3, Alexa Fluor 488-labeled dextran with molecular weight 3000; BSA, bovine serum albumin; CDC, cholesterol dependent cytolysins; CTL, cytotoxic T lymphocytes; DIC, differential interference contrast; DOPC, 1,2-dioleoyl-*sn*-glycero-3-phosphocholine; EGF, epidermal growth factor-like; EGTA, ethyleneglycol-*O*,*O*′-bis(2-aminoethyl)-*N*,*N*,*N*′,*N*′-tetraacetic acid; FD4, FITC-labeled dextran with molecular weight 4000; GUVs, giant unilamellar vesicles; LUVs, large unilamellar vesicles; mABs, monoclonal antibodies; MACPF, membrane attack complex/perforin; NK, natural killer; PFN, perforin; PI, propidium iodide; RU, resonance unit; SPR, surface plasmon resonance.

* Corresponding author. Tel.: +386 1 423 33 88; fax: +386 1 257 33 90.
E-mail address: gregor.anderluh@bf.uni-lj.si (G. Anderluh).
[1] Present address: Institute Jožef Stefan, Jamova cesta 39, 1000 Ljubljana, Slovenia.
[2] These two authors contributed equally to the work.

0161-5890/$ – see front matter © 2010 Elsevier Ltd. All rights reserved.
doi:10.1016/j.molimm.2010.06.001

Author's personal copy

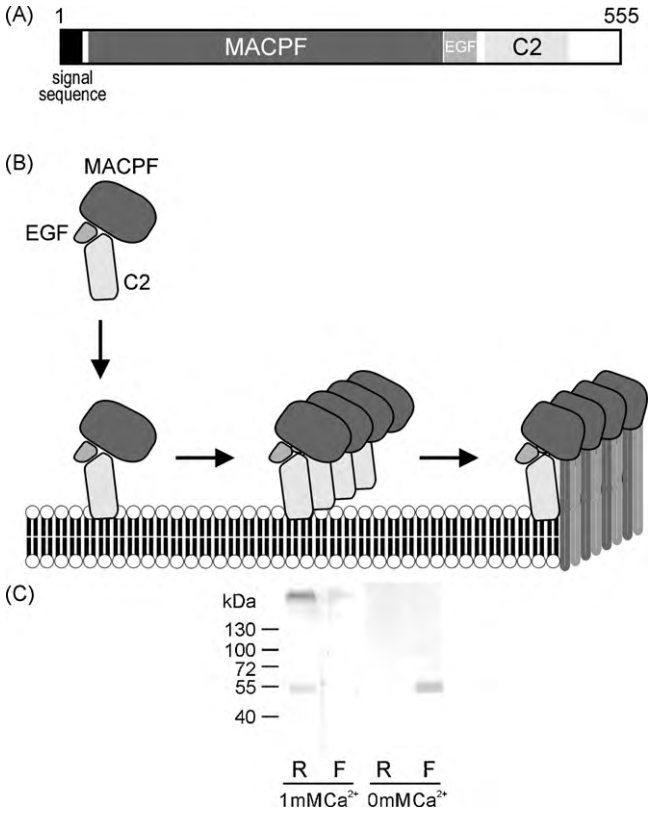

Fig. 1. PFN domain organization and current model of PFN pore formation. (A) PFN is composed of MACPF, EGF and C2 domains. (B) Putative model of PFN pore formation according to functional studies and structural comparisons (Uellner et al., 1997; Voskoboinik et al., 2005; Rosado et al., 2007; Hadders et al., 2007; Baran et al., 2009). Ca^{2+}-dependent membrane binding is achieved by C2 domain (Uellner et al., 1997; Voskoboinik et al., 2005) and is followed by oligomerization on the membrane surface. A pre-pore intermediate forms in CDC and is shown here, by structural analogy, in the middle. However, it was not yet experimentally shown for PFN. The contacts between the monomers are enabled by amino acid side chains from MACPF domain (Baran et al., 2009). Each monomer contributes two β-hairpins to the final β-barrel pore. C, Native human PFN is pure and aggregates in the fluid phase upon Ca^{2+} exposure. One μg of PFN was incubated on ice for 15 min in 1 mM Ca^{2+} or in the absence of Ca^{2+}. PFN was then ultrafiltrated by minicons (Millipore) and the obtained filtrate (F) and retentate (R) precipitated with trichloroacetic acid and everything was loaded onto SDS-PAGE gel. The gel was stained with silver.

presence of a MACPF domain in PFN suggests that it uses a similar mechanism to CDCs to form transmembrane pores (Rosado et al., 2007; Hadders et al., 2007; Anderluh and Lakey, 2008) (Fig. 1B). A major advance in understanding the molecular mechanism of PFN pore formation was achieved recently by identifying crucial amino acid residues that enable oligomerization of PFN after membrane binding (Baran et al., 2009).

The C2 domain at the C terminus is responsible for calcium-dependent binding to the lipid bilayer (Uellner et al., 1997; Voskoboinik et al., 2005) (Fig. 1B). C2 domain has been found in a number of unrelated proteins, e.g. synaptotagmin, protein kinase C-β and phospholipase C-δ. The generic function of the C2 domain in all those proteins is to allow the interaction with the lipid membranes. In some, this is achieved by the coordinated binding of calcium ions, usually through exposed carboxylic groups protruding from loops formed by the β-sheet scaffold (Ponting and Parker, 1996; Nalefski and Falke, 1996; Rizo and Sudhof, 1998). For PFN, the aspartate residues at positions 429, 435, 483, and 485 of the C2 domain are considered essential for calcium-dependent plasma membrane binding (Voskoboinik et al., 2005).

The pore forming activity of PFN is optimal at physiological pH and rapidly diminishes as pH declines such that lytic activity is lost below pH 6.2 (Voskoboinik et al., 2005; Young et al., 1987; Metkar et al., 2005). This protective mechanism minimizes damage to the acidic secretory granules of the cytotoxic cells. The mechanism that restrains PFN activity at acidic pH is uncertain. The protonation of carboxylic groups on aspartate residues within C2 domain has been proposed to reduce the binding of Ca^{2+} and consequently the interactions with cellular membranes (Voskoboinik et al., 2005). However, studies that have examined the pH dependence of PFN activity have focused on permeabilizing activity. It is possible that other steps, apart from the binding to membranes, are influenced by pH during pore formation.

This question is addressed here by using surface plasmon resonance (SPR) and immobilized model membranes. We show that, regardless of pH, PFN monomers readily bind to lipid membranes. Although the binding of PFN to large unilamellar vesicles (LUVs) occurred at neutral and acidic pH, monomers were only desorbed by Ca^{2+} chelation or high salt concentration at pH 5.5. Furthermore, while PFN monomers bound to the model membranes at acidic pH, membrane damage, monitored by the release of a fluorescence probe from chip-immobilized LUVs, was not initiated. These findings were then independently confirmed by fluorescence microscopy that imaged giant unilamellar vesicles (GUVs) and flow cytometry using target cell permeabilization assays. Finally, by using an anti-PFN monoclonal antibody Pf-80 we show that the topology of membrane-associated PFN differed at acidic and neutral pH. Acidic pH thus does not abrogate Ca^{2+} binding or the interaction with lipid membranes. Instead, transition to functional pore is hindered at some other step of pore formation that follows the initial binding.

2. Materials and methods

2.1. Materials

Native human perforin was isolated from secretory granules of YT cells as described (Froelich et al., 1996). This isolation procedure results in pure protein according to silver-stained SDS-PAGE (Fig. 1C). We also found that all pore-forming activity of pure PFN was Ca^{2+} dependent,[3] indicating the absence of contaminating pore-forming proteins from secretory granules, such as granulysin (Stenger et al., 1998), which could interfere with SPR experiments. 1,2-dioleoyl-*sn*-glycero-3-phosphocholine (DOPC) was from Avanti Polar Lipids (USA). Monoclonal antibodies (mAbs) Pf-80 and Pf-344 were from Mabtech (Sweden). Rhodamine B 1,2-dihexadecanoyl-*sn*-glycero-3-phosphoethanolamine, triethylammonium salt (rDHPE) and 3 kDa dextran labeled with Alexa Fluor 488 (AD3), were from Invitrogen (Carlsbad, CA). FITC-labeled antibodies were from Santa Cruz Biotechnology (Santa Cruz, CA). All other chemicals were from Sigma (St. Luis, MO) or Merck (Darmstadt, Germany).

2.2. Preparation of large unilamellar vesicles (LUVs)

DOPC was dissolved in chloroform and dried under vacuum to form a lipid film on the bottom of a glass round flask. The film was resuspended in appropriate buffer by rigorous vortexing in the presence of glass beads. So formed multilamellar vesicles were freeze-thawed six times in liquid nitrogen, followed by extrusion through polycarbonate membranes with 100 nm pores to form LUVs (Anderluh et al., 2005). For calcein release experiments, approximately 60 mM calcein was included in the buffer for preparation of vesicles. Excess dye was removed by gel filtration through

[3] Tilen Praper, Gregor Anderluh and Mauro Dalla Serra, unpublished observation.

Author's personal copy

a small G-50 column. The concentration of the DOPC was measured by using Phospholipids B kit (Wako chemicals GmbH, Germany).

2.3. Binding of PFN to LUVs by SPR

Binding of PFN to the liposomes was determined on Biacore X (Biacore, GE Healthcare) at 25 °C as described (Anderluh et al., 2005). Briefly, the running buffer was always filtered through 0.22 μm filter and degassed. The sensor chip L1 was conditioned with three 1 min consecutive injections of isopropanol/50 mM NaOH (2:3, v/v) before each LUVs deposition. LUVs were immobilized in an appropriate buffer on the surface of the sensor chip to approximately 10 000 response units (RU) at a flow rate of 1 μl/min. The flow rate was then changed to 10 μl/min and the surface was probed by 0.1 mg/ml bovine serum albumin (BSA) solution to assess the completeness of the chip coverage with LUVs. PFN was then injected across LUVs at the same flow rate and the association of PFN was monitored for 1 min and the dissociation for 4 min. The membrane-associated PFN was then probed with various solutions to assess the stability of binding, i.e. 2 mM ethyleneglycol-*O*,*O*′-bis(2-aminoethyl)-*N*,*N*,*N*′,*N*′-tetraacetic acid (EGTA), 1 M NaCl, etc. At the end of the experiment the chip was regenerated by isopropanol/50 mM NaOH (2:3, v/v) solution.

Calcein-loaded LUVs were used to assess the on-chip pore formation of PFN. The buffer coming from the measuring cell, usually between 30 and 50 μl, was collected and diluted in 140 mM NaCl, 20 mM NaH_2PO_4, 1 mM EDTA, pH 7.5 to a final volume of 200 μl. The fluorescence was measured by using a fluorescence microplate reader (Anthos Labtec Instruments GmbH, Austria). The excitation and emission filters were set to 485 and 535 nm, respectively. The percentage of calcein released from the sensor chip was determined by using the following equation:

$$\text{permeabilization}\,(\%) = \frac{F}{\sum F} \times 100,$$

where F and $\sum F$ stand for fluorescence values of the collected particular fraction and sum of fluorescence values of all fractions collected, respectively.

2.4. Epitope mapping

Epitope mapping of mAbs Pf-80 and Pf-344 was performed by blotting of PFN fragments expressed in *E. coli*. Various PFN fragments were either expressed directly in a pET8c-based vector (Kristan et al., 2007) or as TolAIII fusion proteins (Anderluh et al., 2003). Growth of bacteria, induction of protein expression and preparation of whole-cell lysates were done as described previously (Anderluh et al., 2003). Bacterial lysates were resolved on 12% SDS-PAGE gels and Western-blotted. Proteins were transferred to polyvinylidene difluoride membranes (Millipore), blocked overnight in 20 mM Tris–HCl, 150 mM NaCl, pH 7.5 (washing buffer), supplemented with 4% BSA at room temperature. The membrane was washed with the washing buffer and incubated with Pf-80, Pf-344 or anti-Golgin 97 antibodies as a control (Abcam, UK) for 2 h. Bands were stained with secondary antibodies conjugated with horseradish peroxidase by using 4-chloro 1-naphtol and H_2O_2 as a substrate.

2.5. Interaction of mAbs with PFN by SPR

PFN was immobilized on the surface of CM5 chip by amine coupling according to standard procedures of supplier (GE Healthcare Biosciences). PFN rapidly polymerizes in solution when exposed to Ca^{2+} ions at neutral pH (Fig. 1C). We used 10 mM sodium acetate buffer (pH 4.5) supplemented with 5 mM EGTA for immobilization to assure that monomeric PFN was immobilized on the surface of the sensor chip. The interaction of mAbs was assessed in 20 mM HEPES, 150 mM NaCl, 1 mM $CaCl_2$, 0.005% P20 at pH 5.5 or 7.5. The flow rate was 30 μl/min. Various concentrations of antibodies were probed for the interaction with PFN. The association was followed for 60 s and the dissociation was followed for 120 s. The surface was regenerated between cycles by 30 s injection of 20 mM glycine, pH 2.5. The kinetic data were evaluated by 1:1 model, when appropriate, by using Biacore T100 Evaluation Software (Biacore, GE Healthcare Biosciences).

2.6. GUVs electroformation

GUVs were prepared by electroformation as described (Peterlin and Arrigler, 2008) with modifications. The lipids DOPC (for differential interference contrast (DIC) images and immunodetection) or mixture of DOPC and rDHPE at a molar ratio 99:1 (mol/mol; for fluorescence microscopy images) were dissolved in chloroform/methanol (2:1, v/v) to a final 1 mM concentration. 25 μl of the lipid solution was spread onto a pair of Pt electrodes and dried under reduced pressure for 2 h. Electrodes (dimensions: 1 mm, length 34 mm, spacing between electrodes 4 mm) were then placed into a vial filled with sucrose buffer (295 mM sucrose, 1 mM HEPES, 1 mM $CaCl_2$). AC current was applied with a functional generator (GW Instek GFG-3015). The protocol for electroformation was as follows: 2 h of 4 V/10 Hz; 15 min of 2 V/5 Hz; 15 min of 1 V/2.5 Hz; 30 min of 1 V/1 Hz. GUVs were sedimented with the glucose buffer (295 mM glucose, 1 mM HEPES, 1 mM $CaCl_2$). The buffer was then exchanged by gentle pipetting with 150 mM NaCl, 20 mM HEPES, 1 mM $CaCl_2$, pH 5.5 or 7.4 (PFN buffer). GUVs were then divided into aliquots containing approximately equal amount of vesicles.

2.7. Permeabilization of GUVs by PFN

6 μl of GUVs suspension (pH 5.5 or 7.4) was mixed with PFN (6 nM final concentration) or PFN buffer and 0.5 μl of AD3 (0.1 mM final concentration). Mixture was then incubated for 45 min at 25 °C before monitoring the permeabilization by fluorescence microscopy. For activation experiment, 6 μl of GUVs suspension (pH 5.5) was mixed with 0.5 μl of PFN (6 nM final concentration). After 10 min of incubation at 25 °C, GUVs were washed with PFN buffer (pH 5.5) to remove unbound PFN. Sedimented GUVs were then collected from the bottom of the vial and transferred to a new vial containing PFN buffer pH 7.4 and AD3 (0.1 mM final concentration). Mixture was then incubated for another 30 min at 25 °C before fluorescence microscopy. GUVs were considered permeabilized if the fluorescence signal in the interior of the GUV was comparable to the one in the surrounding. GUVs were always individually focused, when they were analyzed for permeabilization.

2.8. Immunodetection of GUVs-bound PFN

6 μl of GUVs suspension (pH 5.5 or 7.4) was mixed with PFN (6 nM final concentration) and incubated for 10 min at 25 °C. Afterwards, 1 μl of anti-PFN δG9-FITC was added and the mixture was incubated for at least 30 min before microscopy. For the isotype control we used anti-glycophorin-FITC labeled antibody (IgG2b isotype). Concentration of antibodies was 200 nM. For activation experiment, 6 μl of GUVs suspension (pH 5.5) was mixed with 0.5 μl of PFN (6 nM final concentration). After 10 min of incubation at 25 °C, GUVs were washed by PFN buffer pH 5.5 to remove unbound PFN. Sedimented GUVs were then collected from the bottom of the vial and transferred to a new vial containing PFN buffer pH 7.4 and anti-PFN δG9-FITC (200 nM final concentration). The mixture was then incubated for another 30 min at 25 °C before fluorescence microscopy.

Author's personal copy

2.9. Fluorescence microscopy

Fluorescence and DIC microscopy was performed on AxioImager Z1 (Carl Zeiss, Germany) equipped with an ApoTome for recording of optical sections (grid-confocal microscopy) and 100 W HBO mercury arc illumination. AD3 and FITC labeled antibodies were observed with 450–490 nm bandpass excitation and 515 nm longpass emission filter. The membranes of the GUVs-containing rDHPE were observed with 546/12 nm bandpass excitation and 590 nm longpass emission filter.

2.10. PFN-mediated target cell permeabilization

Jurkat cells (0.5×10^6) were treated with PFN in presence of the vital dye propidium iodide (PI; 10 μg/ml) at concentrations ranging from 62 to 1500 ng/ml under the following pH conditions:

Set 1: 1.25 mM Ca, 150 mM NaCl, 20 mM HEPES, pH 7.4–0.5% BSA for 30 min at 37 °C.
Set 2: 1.25 mM Ca, 150 mM NaCl, 20 mM HEPES, 0.005% NaN_3, pH 7.4 – 0.5% BSA buffer at 4 °C for 15 min, followed by two washes in 150 mM NaCl, 20 mM HEPES, 0.005% NaN_3, pH 7.4 at 4 °C and finally resuspended in warm 1.25 mM Ca, 150 mM NaCl, 20 mM HEPES, pH7.4, 0.5% BSA. This set was allowed to incubate for 15 min at 37 °C.
Set 3: 1.25 mM Ca, 150 mM NaCl, 20 mM HEPES, 0.005% NaN_3, pH 6 – 0.5% BSA buffer at 4 °C for 15 min, followed by two washes in 150 mM NaCl, 20 mM HEPES, 0.005% NaN_3, pH 7.4 at 4 °C and resuspended in warm 1.25 mM Ca, 150 mM NaCl, 20 mM HEPES, pH 7.4, 0.5% BSA. This set was allowed to incubate for 15 min at 37 °C.
Set 4: 1.25 mM Ca, 150 mM NaCl, 20 mM HEPES, 0.005% NaN_3, pH 6 – 0.5% BSA buffer at 4 °C for 15 min, followed by two washes in 150 mM NaCl, 20 mM HEPES, 5 mM EDTA, 0.005% NaN_3, pH 6 at 4 °C and one wash in 150 mM NaCl, 20 mM HEPES, 0.005% NaN_3, pH 7.4 at 4 °C. Cells were then resuspended in warm 1.25 mM Ca, 150 mM NaCl, 20 mM HEPES, pH 7.4, 0.5% BSA and allowed to incubate for 15 min at 37 °C.

PI was present in all wash buffers. At the end of the incubation, cells were analyzed on a flow cytometer.

3. Results

3.1. Binding of PFN is affected by salt and Ca^{2+} irrespective of pH

In this paper we directly assessed which factors affect the binding of PFN to lipid membranes by employing SPR (Beseničar et al., 2006). In this approach, a stable lipid membrane is prepared on the surface of the sensor chip. The protein of interest is then injected over the membrane and protein-membrane interactions display a signal that reflects larger mass close to the surface of the sensor chip. Under these conditions numerous variables that influence the protein-lipid interaction may be assessed (e.g. running buffer or lipid composition) (Beseničar et al., 2006). For the experiments reported here, the sensor chip L1 was fully covered by immobilizing approximately 10,000 RU of DOPC LUVs. We first investigated the binding of PFN at pH 7.4 to verify that SPR experiments faithfully reproduce other published studies. PFN bound to liposomes stably and irreversibly in the presence of 1 mM Ca^{2+}. Under these conditions, PFN interaction with membranes is dominated by a mass transfer, therefore we did not attempt to determine the kinetic constants for the PFN association with membranes (Fig. 2A). The dissociation of PFN from the immobilized LUVs was minimal indicating the stable association of protein with membranes. In agreement with published data, the binding of PFN to chip immobilized LUVs was negligible in the presence of 2 mM EGTA (Fig. 2A) (Voskoboinik et al., 2005; Uellner et al., 1997; Baran et al., 2009; Tschopp et al., 1989; Young et al., 1987; Ishiura et al., 1990). The binding of PFN was also reduced in the presence of 500 mM NaCl (Fig. 2A), demonstrating the electrostatic component of the membrane interaction. The association of PFN monomers with LUVs at pH 5.5 was qualitatively similar to pH 7.4 (Fig. 2A). It also required mM Ca^{2+} and low salt concentrations, and minimal dissociation of PFN from the membrane was evident in the presence of 1 mM Ca^{2+} (Fig. 2A).

Once the test protein is immobilized, various solutions may be passed over the chip to assess the strength of protein-membrane interaction (Beseničar et al., 2006; Bavdek et al., 2007). We therefore evaluated the general electrostatic interaction as well as the specific influence of calcium ions, after PFN was bound in the presence of 1 mM Ca^{2+} at either pH (Fig. 2B). PFN remained stably bound at pH 7.4 in the presence of either 2 mM EGTA or 1 M NaCl. We also used 100 mM bicarbonate buffer (pH 10.6) or 10 mM glycine–HCl buffer (pH 2.5) for regeneration, but neither solution removed the bound PFN from the membranes,[4] indicating stable membrane association. In comparison, PFN bound to the LUV at pH 5.5 was readily eluted by 2 mM EGTA or 1 M NaCl (Fig. 2B), indicating that PFN binds LUV by electrostatic interactions and that Ca^{2+} ions have a role in the interaction between PFN and LUVs.

We then determined whether a shift from acidic to neutral pH caused PFN to irreversibly associate with the lipid membranes. As shown in Fig. 2B, the signal drops slightly after the injection of buffer with pH 7.4 (denoted by open rectangle in the last row of Fig. 2B), but remaining PFN was stably bound in the presence of either 2 M EGTA or 1 M NaCl. Notably, the observed signal changes were not due to buffer effects on immobilized LUVs. Controls, in the absence of PFN, showed that exposure of LUVs to the corresponding buffers did not reduce the signal and their effects on the liposomes attached to the surface of sensor chip were negligible as shown by gray traces in Fig. 2B.

Collectively these results indicate that Ca^{2+}-dependent binding of PFN to lipid membranes occurs at both pH values studied. Results in Fig. 2 also show that PFN bound at pH 5.5 could be "activated" when the buffer is changed to pH 7.4. The results suggest that the monomers are reversibly bound to the lipid membrane at acidic pH, but then oligomerize and insert into the LUVs when the pH is increased to 7.4, preventing their desorption by EGTA or salt. In comparison, the employed conditions at pH 7.4 should in principle allow the completion of pore formation, hence the stably bound PFN likely represents transmembrane pores. We evaluated this possibility using LUVs loaded with fluorescent marker calcein.

3.2. Bound PFN induces permeabilization of LUV at pH 7.4 and when activated at pH 5.5

Fig. 3A compares the sensorgrams that describe the effect of PFN on LUVs that contain either calcein or buffer in the presence of 1 mM Ca^{2+} at pH 7.4. For the LUVs filled with the fluorophore, the response decreases during the association phase and the response in the dissociation phase is lower than the initial response level before the injection of PFN, reflecting the formation of pores that allow calcein release. To confirm this possibility the fluorescence level was determined in the buffer coming from the measurement cell during the PFN injection (fraction 1 denoted by black rectangle on Fig. 3A) and compared to the fluorescence in the buffer obtained during chip regeneration (fraction 2 in Fig. 3A). Approximately 50%

[4] Mojca Podlesnik Beseničar and Gregor Anderluh, unpublished observation.

Author's personal copy

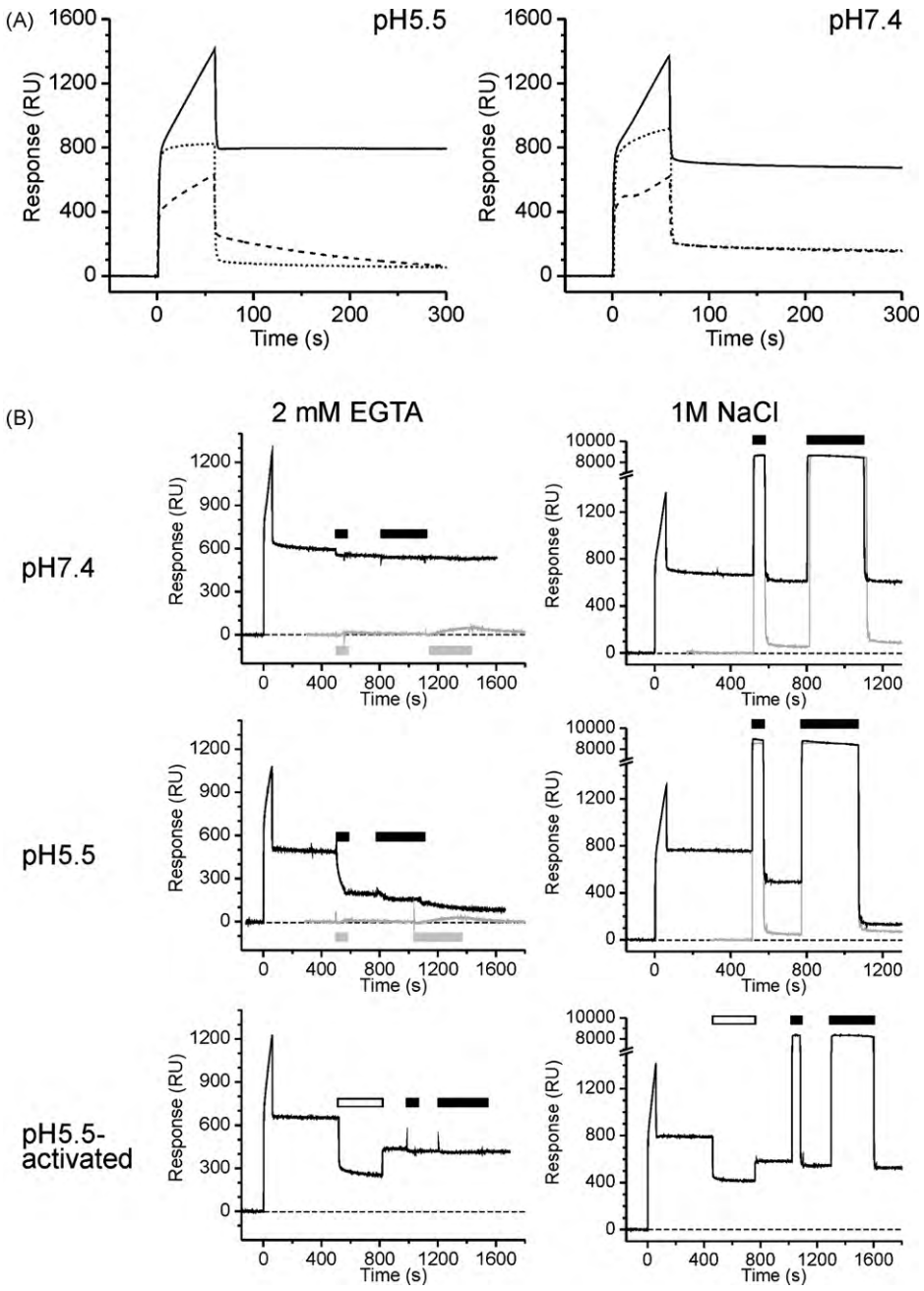

Fig. 2. PFN binding to membranes is affected by salt and Ca^{2+} ions irrespective of pH. In all panels the flow-rate was 5 μl/min and experiments were performed at 25 °C. (A) Binding of approximately 50 nM PFN to an L1 sensor chip covered with DOPC LUV at indicated pH values. The buffers used were: 20 mM HEPES, 150 mM NaCl, 1 mM $CaCl_2$ (solid line); 20 mM HEPES, 500 mM NaCl, 1 mM $CaCl_2$ (dashed line); 20 mM HEPES, 150 mM NaCl, 2 mM EGTA (dotted line). (B) Removal of bound PFN from the LUV by subsequent injections of 2 mM EGTA or 1 M NaCl. EGTA or NaCl were injected for 1 or 5 min as indicated by black rectangles. The dashed line denotes the response value before the injection of PFN, i.e. it corresponds to the signal of LUV on the sensor chip. The gray traces show responses obtained in the absence of PFN. The bound PFN at pH 5.5 was activated by a single 5 min injection of the same buffer with pH 7.4 (empty rectangle) (see also Fig. 3).

of the total fluorescence resided in the buffer that followed PFN injection (Fig. 3C) confirming that substantial calcein was released when PFN associates with LUV and that the decrease in the signal is attributable to calcein released from the liposomes. We did not observe release of calcein from chip-immobilized LUVs in the presence of millimolar concentrations of EDTA,[5] in agreement with the observation that PFN does not bind to chip-immobilized LUVs in the presence of the chelator (Fig. 2A).

To ensure that calcein release is due to the leakage from the liposomes rather than the release of vesicles from the sensor chip, we also measured fluorescence of fractions in the presence of Triton X-100. Calcein was encapsulated in the liposomes at self-quenching concentration (around 60 mM). The presence of detergent should release all of the encapsulated calcein and fluorescence should consequently increase. However, there were no differences in the absence or presence of detergent, indicating that calcein escaped through PFN generated pores.

The sensorgram that described PFN binding to calcein-loaded LUVs at pH 5.5 was indistinguishable from the signal obtained for

[5] Mojca Podlesnik Beseničar and Gregor Anderluh, unpublished observation.

Author's personal copy

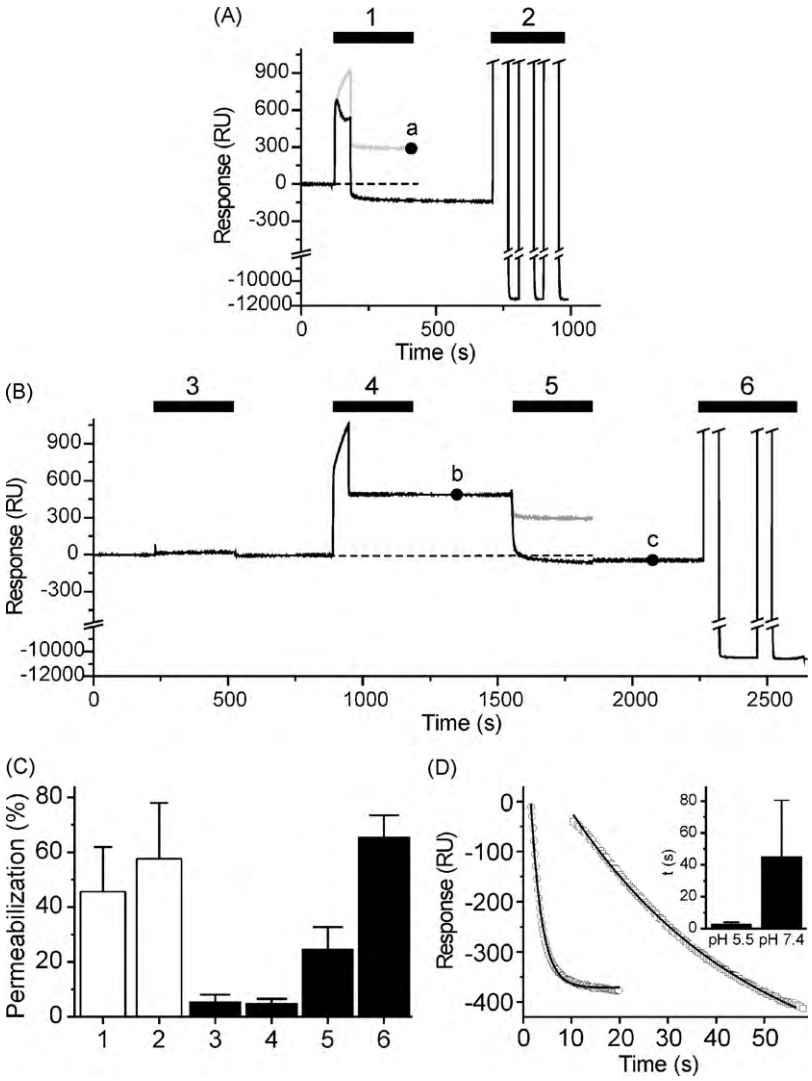

Fig. 3. Bound PFN permeabilizes calcein-loaded LUV at pH 7.4 and when activated at pH 5.5 by increasing a pH to 7.4, but not at pH 5.5. The experimental conditions are as in Fig. 2. (A) Sensorgram of PFN binding to an L1 sensor chip covered with liposomes loaded with fluorescent probe calcein at pH 7.4. The sensorgram of PFN binding to DOPC liposomes without calcein is shown by a gray line for the comparison. The buffer was collected within time intervals, indicated by black rectangles, and fluorescence was measured subsequently by a fluorimeter. The dashed line represents a response level before PFN injection. Responses are trimmed for clarity at the end of experiment. Rectangle 1, injection of PFN; rectangle 2, injection of 50 mM NaOH: isopropanol 2:3 in order to remove the remaining vesicles and regenerate sensor chip. (B) The same experiment as in A, but performed at pH 5.5. Rectangles 3 and 5, injection of 20 mM HEPES, 150 mM NaCl, 1 mM $CaCl_2$, pH 7.4; rectangle 4, injection of PFN; rectangle 6, injection of 50 mM NaOH: isopropanol 2:3. The black dots with small letters in (A) and (B) denote times when the surface of the chip was probed in independent experiments by monoclonal antibodies. These results are presented in Fig. 7. (C) Intensity of fluorescence of samples 1–6. The permeabilization is represented as a fraction of all fractions collected for each pH value. $n = 5–6$; average ± S.D. (D) The rate of permeabilization is faster when PFN prebound at pH 5.5 is activated than when assayed at pH 7.4. The sensorgams in the absence of calcein in LUV (gray in Fig. 3) were subtracted from sensorgrams in the presence of calcein (black in Fig. 3) to obtain the signal change that is due to changes of calcein mass concentration near the surface of the sensor chip. Circles, activation of prebound PFN by injection of pH 7.4 buffer (i.e. rectangle 5 in Fig. 3); squares, PFN injected at pH 7.4 (rectangle 1 in Fig. 3). The obtained responses were fitted to a mono-exponential decay and time constant is reported in the inset. $n = 3$; average ± S.D.

LUVs without calcein (Fig. 3B), indicating that the fluorophore was not released from LUVs at this acidic pH. The fluorescence of the buffer eluted from the measurement cell was negligible thus confirming this interpretation (fraction 4 in Fig. 3B). However, when the pH was raised to 7.4 (i.e. pH activation) (fraction 5 in Fig. 3B), calcein release was apparent (Fig. 3C), indicating that functional pores are formed at the surface of LUVs. The control injection of the buffer across intact calcein-loaded LUVs surface (fraction 3 in Fig. 3B) did not release calcein. The subtraction of sensorgrams that depicts PFN binding to calcein-filled LUVs from the sensorgrams for PFN bound to buffer-filled vesicles defines the rate of PFN-dependent calcein release (Fig. 3D). In comparison to the rate of permeabilization observed following the injection of PFN across calcein-filled vesicles at pH 7.4, the rate of calcein release was greater when PFN was first bound to the surface of LUVs at pH 5.5 and then activated by injection of pH 7.4 buffer (inset in Fig. 3D).

3.3. PFN binding to GUVs is pH-independent while permeabilization only occurs at pH 7.4

We next examined the permeabilization of GUVs by PFN at pH 7.4 or 5.5 by monitoring the influx of Alexa488 labeled dextran (MW = 3 kDa; AD3). After 45 min at room temperature, almost all GUVs were permeabilized at pH 7.4, while the GUVs remained intact at pH 5.5 (Fig. 4A and B). In the absence of PFN, the spontaneous diffusion of AD3 into the GUVs was insignificant (Fig. 4A and B).

The binding of PFN to GUVs was assessed by using fluorescently labeled anti-PFN δG9 antibodies. PFN was readily detected

Author's personal copy

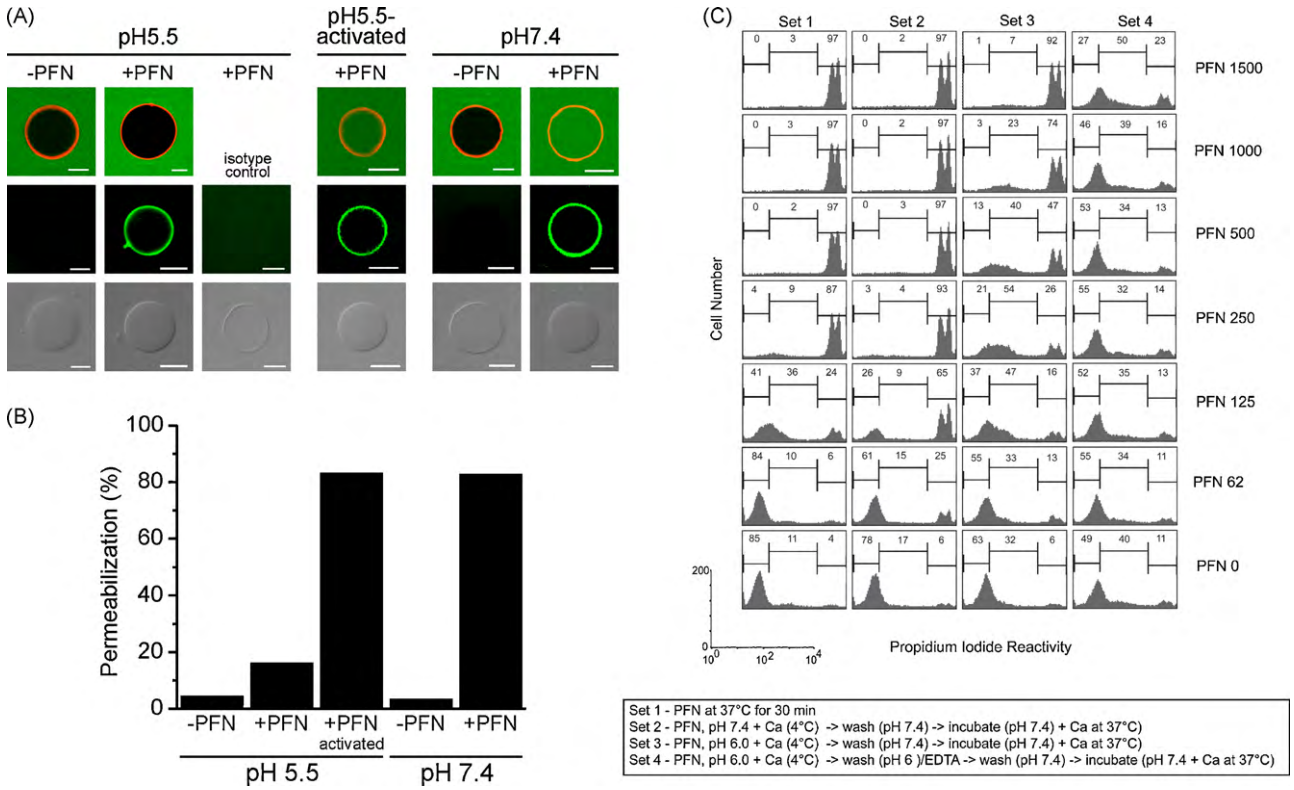

Fig. 4. PFN binds GUVs at pH 5.5, but permeabilizes them at pH 7.4 or upon activation of PFN prebound at pH 5.5. (A) Permeabilization of GUVs and immunodetection of membrane-bound PFN. The top row shows GUVs with membrane labeled by rDHPE (red) incubated with (PFN+) or without PFN (PFN-) and fluorescent dextran AD3 (green) in the surrounding medium. The middle row shows fluorescence of anti-PFN δG9-FITC labeled antibody. The bottom row shows DIC images of the GUVs in the middle rows. Concentrations were 6 nM, 200 nM and 0.1 mM for the PFN, monoclonal antibodies and AD3 respectively. The antibody used for the isotype control was anti-glycophorin-FITC labelled antibody and was used at the same concentration. Buffer was 150 mM NaCl, 20 mM HEPES, 1 mM $CaCl_2$, pH 5.5 or 7.4 (as indicated). Scale bar is 10 μm in all panels. (B) Proportion of permeabilized GUVs by PFN at different experimental conditions explained in A. GUVs were considered as permeabilized if the fluorescent signal in the interior of the GUV was approximately equal as in the surrounding. In total, we analyzed 30–113 GUVs for individual experimental condition. *C*, Permeabilization of Jurkat cells under varying pH conditions. Cells were treated with PFN at the indicated concentrations in four sets under conditions summarized in the text box below the histograms. Cells were analyzed by flow cytometry and the numbers in histograms represent the % events in the respective regions. Data is representative of one of two independent experiments.

on the surface of the GUVs regardless of pH (Fig. 4A). GUVs were not stained by anti-PFN δG9 in the absence of PFN. To verify that the interaction of the δG9 mAb with GUV membrane at acidic pH was not due to electrostatic effects, we performed the same experiments using FITC labeled anti-glycophorin labeled antibody as an isotype control. The isotype control antibody did not interact with GUVs membranes in either the presence or absence of PFN (Fig. 4A).

We have also performed the "activation" experiment described in the SPR system. PFN was allowed to undergo Ca^{2+}-dependent binding to the GUVs at pH 5.5. The vesicles were then washed and pH was increased to 7.4. The bound PFN retained the capacity to permeabilize the vesicles, similar to GUVs exposed to PFN at pH 7.4 (Fig. 4A and B) and thus faithfully reproduced the results observed by SPR. Overall, the δG9 mAb specifically recognizes PFN bound to the GUVs. δG9 mAb appears to be directed toward an epitope that remains accessible when PFN undergoes Ca^{2+}-dependent binding to membrane vesicles as well as when the monomers oligomerize and insert to form a transmembrane pore.

3.4. PFN bound at pH 6 could be activated by rise in pH in Jurkat cells

Finally, we examined how the immobilization of the PFN monomers to the plasma membrane of Jurkat cells influenced the permeabilization. In comparison to the standard approach, in which target cells are incubated with soluble PFN at 37 °C (set 1), the cells were incubated at pH 7.4 in the presence of calcium at 4 °C, then washed (4 °C) and the temperature of the cells elevated to 37 °C (set 2). Target cells were also incubated with PFN in acidic buffer (pH 6.0) in the presence of mM calcium and washed either in the absence (set 3) or presence of 5 mM EDTA (set 4) followed by incubation at 37 °C. In all instances, PI, added at the onset of the incubation, was used to estimate membrane damage. Regardless of pH chosen to immobilize the PFN monomers, permeabilization of the target cells was apparent (Fig. 4C, set 2 and 3). Calcium was essential for permeabilization because its chelation prevented membrane damage (set 4). Interestingly, at pH 7.4, immobilized rather than soluble PFN was more active (Fig. 4C, sets 1 and 2).

3.5. mAbs Pf-80 and Pf-344 as a tool to study conformation of PFN

We examined the utility of Pf-80 and Pf-344 mAbs (Zuber et al., 2005, 2006) to elucidate the conformational states of membrane-bound PFN at different pH values. First we characterize epitopes that both antibodies recognize by using PFN fragments expressed in *E. coli* (Fig. 5). The epitope recognized by the Pf-344 mAb mapped between amino acids 373–388. These amino acids span the end of MACPF domain to the start of the EGF-like domain (Fig. 5). Pf-80 has been reported to recognize a conformational epitope possessed by PFN that is stored in cytotoxic granules and which cross-competes with the δG9 mAb (Zuber et al., 2005). In agreement with this report, the Pf-80 mAb failed to react with all fragments expressed for epitope mapping study (Fig. 5).

Author's personal copy

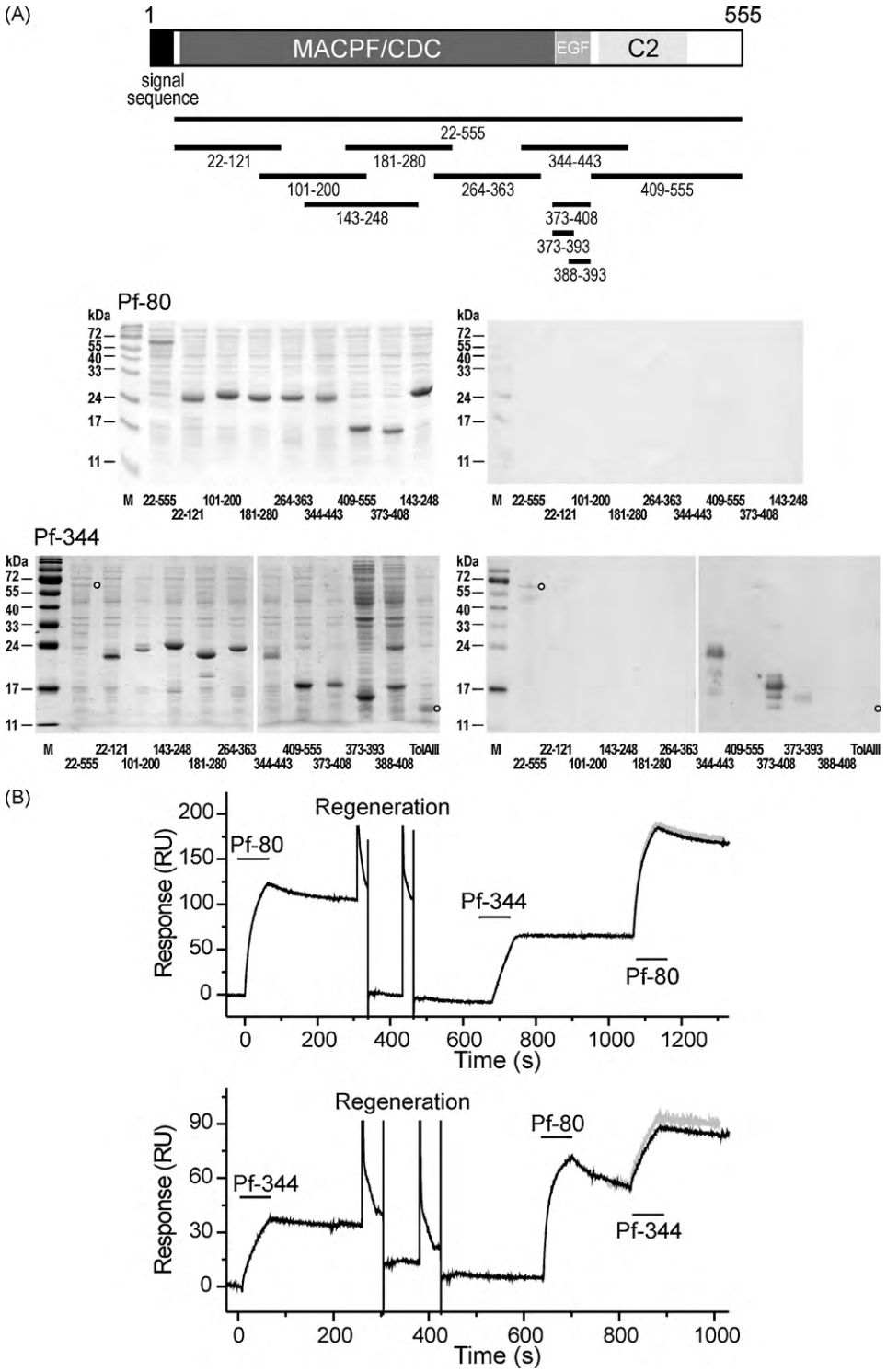

Fig. 5. mAb Pf-80 recognizes conformational epitope, while Pf-344 binds EGF-like domain within region 373–388. (A) Human perforin is schematically presented on the top. Different domains are shaded black or gray. The fragments used in mapping of epitopes are shown below. Numbers denote the beginning and end of each fragment, according to the numbering of the precursor PFN. PFN fragments were expressed in *E. coli* and resolved on SDS-PAGE gels and stained with Coomassie blue (below left) or blotted (below right). The fragments that were used for each antibody are indicated below the gel or blot. The whole length PFN was poorly visible in the gel of Pf-344 and its position is shown by a circle on the gel and blot. Circle denotes also the position of negative control TolAIII. Some degradation products may be seen in the blots. (B) mAbs Pf-80 and Pf-344 bind to non-overlapped epitopes. The experiment was performed in 20 mM HEPES, 150 mM NaCl, 1 mM $CaCl_2$, 0.005% P20, pH 7.4. Approximately 1200 RU of monomeric PFN was immobilized via amino groups on the surface of CM5 chip. mAbs at 100 nM concentration were injected as denoted. The surface was regenerated between different injections by 1 min pulses of 10 mM glycine, pH 2.5. The second injection of the same antibody is overlaid by the first injection (in gray) for the comparison.

The capacity of the two mAbs to recognize monomeric PFN was then assessed. PFN was immobilized to the surface of CM5 sensor chip in the presence of EGTA to ensure that all immobilized PFN was in monomeric form. Both mAbs at 100 nM concentration recognized immobilized PFN in monomeric form in the presence of 1 mM Ca^{2+} (Fig. 5B). Furthermore, the mAbs appeared to recognize spatially distant epitopes because cross-competition was not evident (Fig. 5B). Next, we assessed the interaction of the mAbs

Author's personal copy

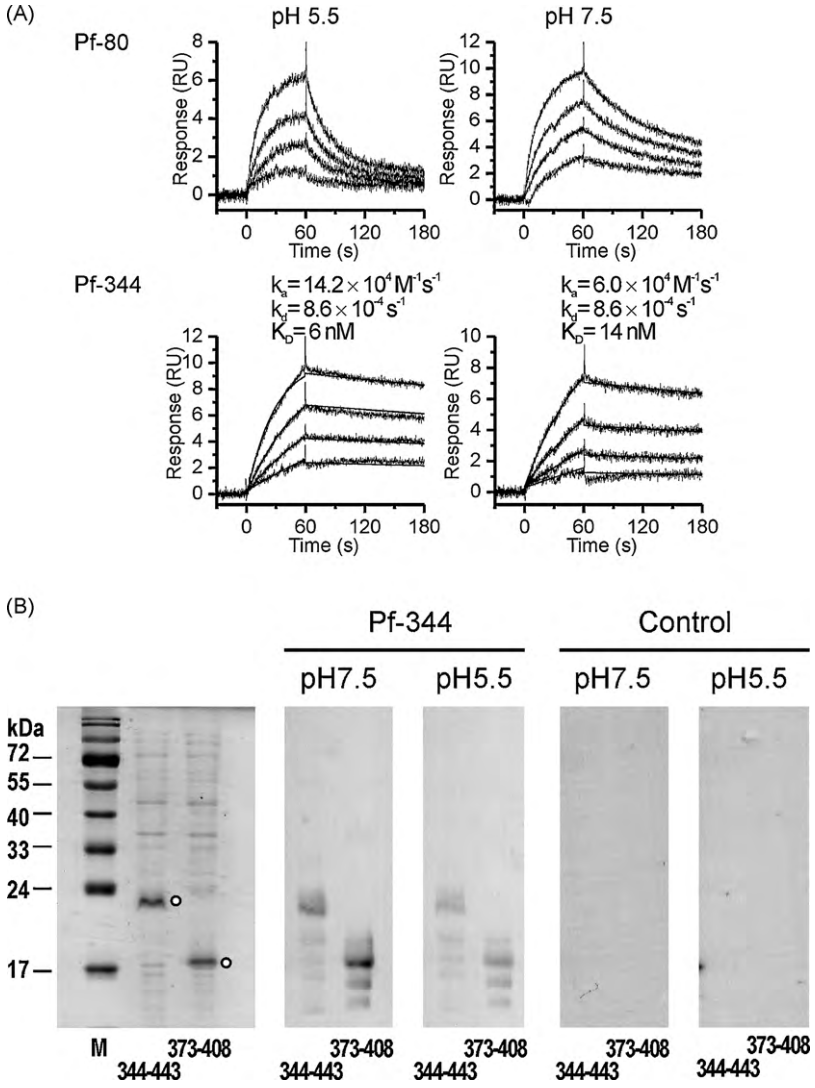

Fig. 6. Binding of mAbs to PFN is not affected by pH. (A) SPR analysis of mAb binding to monomeric human PFN. PFN was immobilized via amino groups on the surface of CM5 chip to approximately 60 RU. The concentrations of antibodies were 31.3, 62.5, 125 and 250 nM in all cases (from bottom to top). The flow-rate was 30 μl/min. The data for Pf-344 could be fitted to 1:1 binding model (shown by black lines) and obtained kinetic constants are reported by the sensorgrams. (B) Binding of Pf-344 to PFN fragments at two different pH values. Membranes with PFN fragments were incubated in buffers with indicated pH values with Pf-344 or control antibody (anti-Golgin 97). The gel is shown on the left for the comparison with recombinant PFN fragments indicated by circles.

with PFN at acidic pH 5.5 and at pH 7.4 (Fig. 6). Sensorgrams indicate that binding is pH independent. The Pf-344 mAb interaction with the immobilized PFN could be fitted to a 1:1 binding model, revealing an equilibrium binding constants in nM range for both pH values (Fig. 6A). The binding of Pf-80 to PFN was complex and the 1:1 model could not be used to describe the protein-protein interaction, but it was clear from the sensorgrams that the Pf-80 mAb robustly bound to PFN at either pH (Fig. 6A). The binding of Pf-344 at two pH values was assessed also by Western blot, where fragments containing epitope of Pf-344 could be easily stained by the antibody (Fig. 6B). In summary, we show that epitopes of Pf-80 and Pf-344 do not spatially overlap and that recognition of PFN by both antibodies is not affected by pH.

3.6. mAbs Pf-80 and Pf-344 recognize membrane-associated PFN

We have used mAbs to determine the exposure of epitopes of membrane associated PFN at three different conditions. Specifically, PFN exposed to immobilized LUVs at pH 7.4 and 5.5 as well as monomers that had undergone Ca^{2+}-dependent binding to the vesicles at acidic pH and then transitioned to pH 7.4 (Fig. 7; the small capital letters on sensorgrams of Fig. 3 highlight when membrane-bound PFN was probed for the binding of antibodies). The binding of antibodies to the liposomes in the absence of PFN was negligible and was used as a control and subtracted from the responses in the presence of PFN. The binding of Pf-344 was comparable for the three conditions. Pf-80 reacted poorly with PFN monomers at pH 7.4 and when PFN was activated by pH. In comparison, the Pf-80 reacted quite robustly to PFN monomers that had been adsorbed to the LUVs in the acidic buffer containing Ca^{2+} (Fig. 7).

Antibody recognition of membrane-associated PFN indicates that epitopes of both antibodies appear not to be involved in membrane-binding step. To evaluate this hypothesis, PFN was incubated with each mAb in a molar ratio 1:20 on ice for 20 min and then assayed for the association with the membranes. The responses of the complex PFN-mAb were much higher in comparison to responses of PFN alone (Fig. 8A), as a result of the additional mass provided by the mAb bound to the PFN. The complex mAb-PFN thus retained capacity to interact with the membrane and bound efficiently.

Author's personal copy

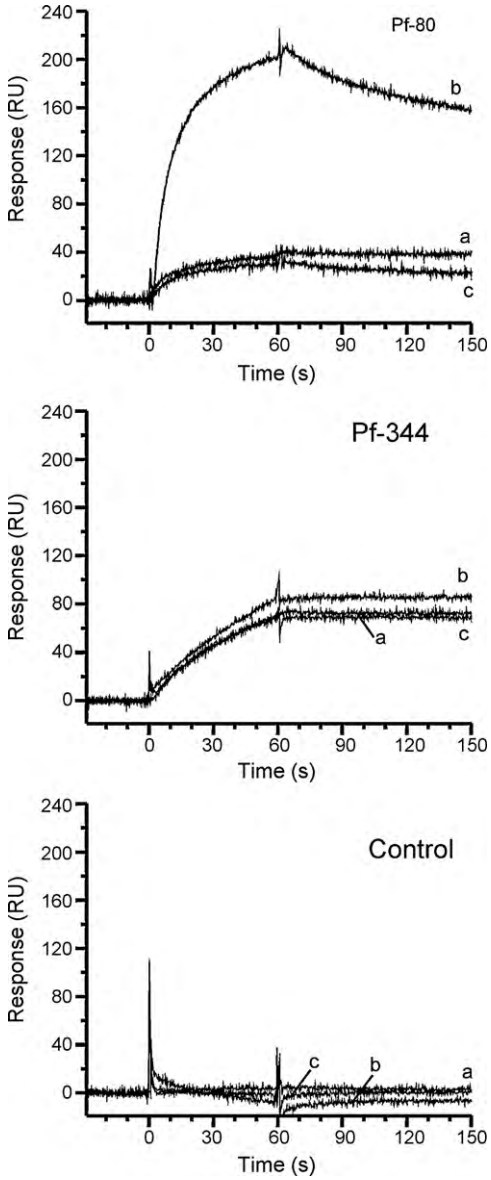

Fig. 7. mAbs recognize membrane-associated PFN. Binding of mAbs to various forms of PFN on the surface of DOPC LUV. Antibodies at 500 nM concentration in the running buffer were injected after PFN binding experiment was performed. The designations on the sensorgrams correspond to different conditions as highlighted in Fig. 3, i.e. a, PFN bound at pH 7.4; b, PFN bound at pH 5.5 and c, PFN bound at pH 5.5 after activation with the pH 7.4 buffer. Other experimental conditions were as in Fig. 2.

The results on Fig. 7 indicate that epitope for antibody Pf-80 is not accessible in vesicles where PFN has formed transmembrane pores, while the region recognized by mAb Pf-344 is exposed regardless of PFN conformational state. The binding of Pf-80 to the PFN is predicted to affect either the oligomerization of the monomers at the surface of the LUVs or subsequent steps in the pore forming process. To evaluate this possibility, we injected mAb-PFN complexes across the immobilized LUVs followed by EGTA injection to deplete Ca^{2+} ions. Calcium chelation did not affect PFN that was preincubated with Pf-344 or control antibody, but desorbed almost completely PFN that was preincubated with Pf-80 mAb (Fig. 8B), indicating that the Pf-80 mAb drastically affects how the monomers interact with the membrane after initial binding.

We then asked whether the Pf-80 disrupted the pore formation by monitoring the permeabilization of GUVs for FITC-labeled 4 kDa dextran (FD4). PFN (12 nM) caused substantial membrane damage, while preincubation of PFN with Pf-80 mAb dramatically reduced GUV permeabilization (Fig. 8C and D). The Pf-344 mAb did not similarly influence PFN activity, since it did not have any effect on the permeabilization ability of the PFN. The permeabilization of GUVs in the absence of PFN or in the presence of mAbs without PFN was minimal (Fig. 8C and D).

The Pf-80 and Pf-344 mAbs therefore appear to recognize different membrane-associated conformational states of PFN. While neither mAb influence the binding of PFN monomers to the model membranes, the epitope recognized by the Pf-344 mAb remains exposed throughout the various steps in the pore formation, while Pf-80 mAb recognizes an epitope that is involved in steps of pore formation that follow initial binding.

4. Discussion

Despite the intense research in the last two decades, the structural and functional characteristics of PFN are still elusive and not understood sufficiently to explain its mechanism of membrane association and pore formation (Voskoboinik et al., 2006; Pipkin and Lieberman, 2007). In this paper, we have relied on the versatility of SPR and GUV imaging to study the membrane interaction of native human PFN. Specifically, the effects of calcium ions and pH on LUV-associated PFN were explored and the utility of two recently described anti-PFN mAbs (Zuber et al., 2005) to dissect the binding, oligomerization, insertion and transmembrane pore formation was assessed. The presented results clearly show that the interaction of PFN with the lipid membranes includes electrostatic interaction that is followed by the oligomerization and insertion, which finally results in firmly bound protein.

To ensure that PFN does not inadvertently damage its host, the expression, targeting and storage of this highly potent pore forming protein in a cytotoxic cell is precisely regulated and restrained with self-protection implemented at multiple levels. PFN is expressed as an inactive precursor (Uellner et al., 1997), which binds to calreticulin (Fraser et al., 2000) and transports to cytotoxic granules (Peters et al., 1991). PFN is then activated by a proteolytic cleavage. Its activity in granules is minimized by calreticulin, which chelates Ca^{2+} ions, and by the granule-associated proteoglycan serglycin, which binds to PFN and prevents its oligomerization (Metkar et al., 2002). Additional level of protection is low pH of granules, which inhibits lytic activity of PFN (Young et al., 1987; Metkar et al., 2005; Voskoboinik et al., 2005).

We show that the binding of PFN at acidic (5.5) and neutral pH (7.4) to membrane lipids is absolutely dependent on Ca^{2+}, a process mediated by aspartate residues located on the C2 domain (Voskoboinik et al., 2005). The average pK_a value for aspartate residues in proteins is 3 (Forsyth et al., 2002; Grimsley et al., 2009). Although the higher pK_a values for negatively charged amino acid residues in proteins were also observed (in less than 5% of acidic residues for which pK_a values were determined), they were mostly found in the interior of the protein forming active sites (Forsyth et al., 2002). It is not known how the local environment (pH) or membrane proximity influences the pK_a values of the aspartate residues that bind Ca^{2+} ions. The affinity of PFN for calcium remains to be determined for different pH values, but it is likely that the aspartates on the C2 domain are not protonated at pH 5.5. However, PFN is not firmly inserted at pH 5.5, while at pH 7.4 it is irreversibly associated with the membrane and cannot be removed from the membrane by calcium chelation or other treatments used to regenerate membrane surfaces in protein–membrane interactions studies by SPR (Besenič ar et al., 2006). This notion is in agreement with observation of Ishiura et al., who showed that majority of membrane bound perforin at neutral pH was firmly associated with red blood cells membrane, resisting elution by EDTA wash (Ishiura et al., 1990).

Author's personal copy

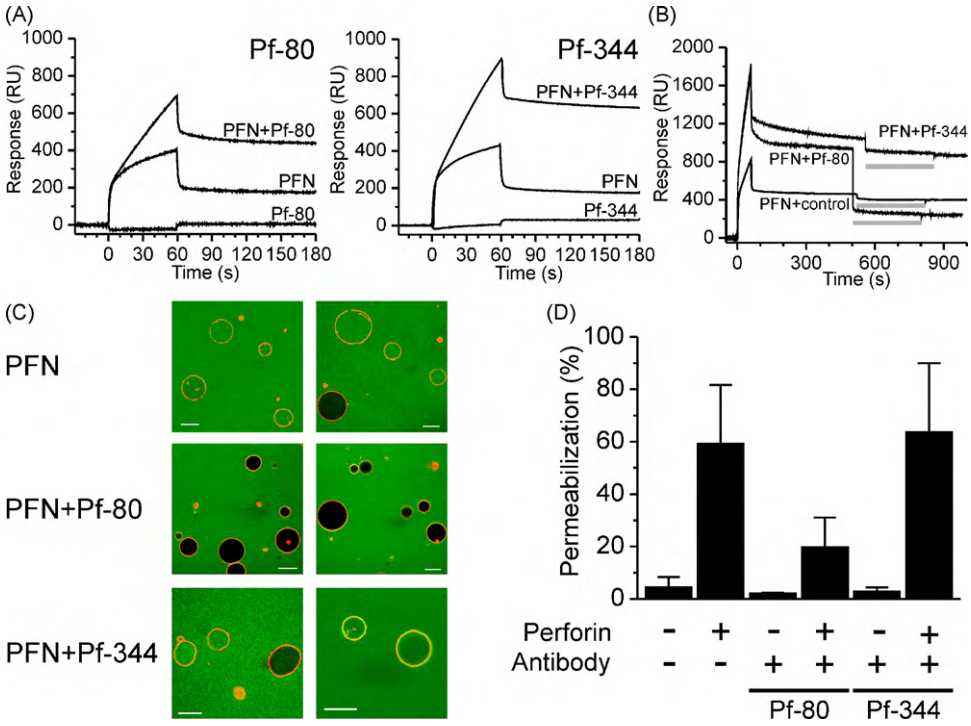

Fig. 8. Binding of mAbs to PFN does not prevent binding, but oligomerization in the case of Pf-80. The buffer used was 20 mM HEPES, 150 mM NaCl, 1 mM $CaCl_2$, pH 7.4. Other experimental conditions were as in Fig. 2. (A) PFN at approximately 20 nM final concentration was injected across DOPC-covered sensor chip (PFN). The same amount was also preincubated with mAbs at the molar ratio PFN:mAbs 1:20 for at least 20 minutes on ice and then injected across the chip (PFN + mAbs). The injection of antibody without PFN is also shown. (B) PFN was preincubated with mAbs as above and then injected across the DOPC-covered sensor chip at the final 50 nM concentration. The stability of bound PFN was assessed subsequently with 5 min injection of 20 mM HEPES, 150 mM NaCl, 2 mM EGTA, pH 7.4 (as indicated by the gray line). As a control PFN was preincubated with control antibody (anti GM-130 mAbs). (C) GUVs were exposed to PFN or PFN pre-incubated with mAbs at a molar ratio 1:20 for 20 min on ice and then assessed for the permeabilization. Scale bar is 20 μm in all panels. (D) Quantification of permeabilization as presented in (C). The concentration of PFN was 12 nM. The data presented are average of 4–7 experiments ± S.D. In total 130–239 vesicles were analyzed.

We suspect that the acidic environment prevents progression to the pore forming state. This possibility is exemplified by showing that the membrane-bound PFN is not lytic at pH 5.5, according to SPR-based assay (Fig. 3) and GUVs experiments (Fig. 4), but it is possible to activate it simply by raising pH of the buffer, while keeping the salt and calcium ions unchanged (Figs. 3 and 4). We have also performed experiment on Jurkat cells and confirmed this novel pH activation mechanism at the cellular level, thus showing its physiological relevance. The experiment on Jurkat cells also revealed a distinct subset of cells with low PI reactivity (set 3 on Fig. 4C). The importance of this subset of cells for perforin activity *in vivo* remains to be determined. Furthermore, a comparison of PFN mixed with Jurkat cells in solution versus pre-bound at neutral pH and low temperature indicated that the latter appeared to be more active on concentration basis (Fig. 4C). This may be attributable to the rapid inactivation of PFN by the fluid phase-associated calcium at 37 °C (Kataoka et al., 1997),[6] but also to the formation of pre-pore forms at low temperature, which transition readily to pore states at higher temperature.

The SPR experiment also allowed determining the kinetics of calcein efflux from chip-immobilized liposomes. The kinetics of calcein release at pH 5.5 is faster in comparison to the release at physiological pH, implying that some of the steps in PFN pore formation were already completed, e.g. binding to the membranes, and perhaps protein may even exist in loosely associated oligomeric form. Conceptually similar result was obtained with the disulfide mutant of CDC perfringolysin, which did not cause hemolysis due to the disulfide formation that prevented completion of the pore forming process and locked protein in the non-lytic prepore state. However, upon activation with dithiothreitol the kinetics of the hemolysis was much faster than in the wild-type protein (Heuck et al., 2000).

The results altogether suggest that acidic pH influences steps in the pore forming mechanism beyond membrane binding. R213 and E343 on adjacent monomers of the MACPF domain were found to form a salt bridge during the oligomerization of PFN (Baran et al., 2009). The pK_a values for glutamate residues are approximately one unit higher than those of aspartate residues (Forsyth et al., 2002; Grimsley et al., 2009), thus the acidic pH 5.5 would result in protonation of E343 residue impairing formation of the salt bridge and possibly oligomer formation (Baran et al., 2009), while aspartate residues on C2 domain responsible for Ca^{2+} binding are unaffected.

The state of the protein at the surface of the membrane is different at two studied pH values according to experiments with mAbs We studied the influence of Pf-80 and Pf-344 mAbs on the binding of PFN monomers, as well as subsequent steps in pore formation (Fig. 7). Since Pf-344 binds to PFN region 373–388 remote to the membrane-interacting C2 domain, membrane binding is predicted and was shown to be unaffected by this mAb (Fig. 8). Similarly, Pf-80 does not appear to recognize an epitope that contributes Ca^{2+}-dependent binding through C2 domain. However, this antibody decouples membrane binding from the steps that lead to pore formation (Fig. 1). Although permeabilization of GUVs was lower, if PFN was preincubated with Pf-80 (Fig. 8), the binding of PFN monomers to the model membranes was unaffected (Fig. 7), suggesting that the Pf-80 mAb interacts with a conformational epitope that participates in oligomerization at the membrane plane or pos-

[6] Sunil Metkar and Christopher J. Froelich, unpublished observation.

Author's personal copy

sibly during insertion of the oligomerized monomers. Accordingly, in the presence of Pf-80, bound PFN could be removed by EGTA (Fig. 8B). The experiments presented in Fig. 8 are thus important for the interpretation of the SPR data presented in Fig. 2, since we indirectly prove that oligomerization and pore formation by PFN on the surface of the LUVs enables stable PFN association. Thus, among the mAbs we have tested, the Pf-80 may be useful to treat PFN-mediated immunopathology.

Effector molecules are released into the immunological synapse from the secretory granules. They consist of the dense core where the serglycin-bound PFN and granzyme are located (Masson et al., 1990) and peripheral multivesicular cortex containing the lysosomal proteins (Burkhardt et al., 1990). The pH of the multivesicular domain was estimated to be 5.4–5.5. The pH of the dense core where the PFN is located is presumably slightly higher (Burkhardt et al., 1990) but still acidic since the shifting of the pH to neutral inactivates the PFN stored in the granules (Kataoka et al., 1997). It has been shown that the pH 5.5 protects PFN from the inactivation in the presence of high calcium concentration (Kataoka et al., 1997). Immunological synapse between the effector and the target cell is a very tight compartment (Stinchcombe et al., 2001; Clark et al., 2003; McCann et al., 2003), so the pH in the extracellular space between effector and the target cell might be slightly altered by the low pH of the lytic granules after degranulation. After secretion PFN dissociates from serglycin (Masson et al., 1990) with two possible outcomes. The presence of Ca^{2+} in the fluid phase causes its rapid aggregation and inactivation. On the other hand calcium ions enable binding to the target cell plasma membrane. The ability of PFN to associate with membranes regardless of pH may aid to avoid the inactivation in the high calcium extracellular medium.

Acknowledgements

We would like to acknowledge the expert help of Vesna Hodnik. The Slovenian authors would like to acknowledge the support of the Slovenian Research Agency (programme grant P1-0207 and the Slovenian–USA bilateral collaborative grant). C. J. F. was supported through 5RO1AI04494-03 of the NIAID.

References

Anderluh, G., Beseničar, M., Kladnik, A., Lakey, J.H., Maček, P., 2005. Properties of nonfused liposomes immobilized on an L1 Biacore chip and their permeabilization by a eukaryotic pore-forming toxin. Anal. Biochem. 344, 43–52.

Anderluh, G., Gokce, I., Lakey, J.H., 2003. Expression of proteins using the third domain of the Escherichia coli periplasmic-protein TolA as a fusion partner. Protein Exp. Purif. 28, 173–181.

Anderluh, G., Lakey, J.H., 2008. Disparate proteins use similar architectures to damage membranes. Trends Biochem. Sci. 33, 482–490.

Baran, K., Dunstone, M., Chia, J., Ciccone, A., Browne, K.A., Clarke, C.J., Lukoyanova, N., Saibil, H., Whisstock, J.C., Voskoboinik, I., Trapani, J.A., 2009. The molecular basis for perforin oligomerization and transmembrane pore assembly. Immunity 30, 684–695.

Bavdek, A., Gekara, N.O., Priselac, D., Gutiérrez, Aguirre, I., Darji, A., Chakraborty, T., Maček, P., Lakey, J.H., Weiss, S., Anderluh, G., 2007. Sterol and pH interdependence in the binding, oligomerization, and pore formation of Listeriolysin O. Biochemistry 46, 4425–4437.

Beseničar, M., Maček, P., Lakey, J.H., Anderluh, G., 2006. Surface plasmon resonance in protein-membrane interactions. Chem. Phys. Lipids 141, 169–178.

Burkhardt, J.K., Hester, S., Lapham, C.K., Argon, Y., 1990. The lytic granules of natural killer cells are dual-function organelles combining secretory and pre-lysosomal compartments. J. Cell Biol. 111, 2327–2340.

Clark, R.H., Stinchcombe, J.C., Day, A., Blott, E., Booth, S., Bossi, G., Hamblin, T., Davies, E.G., Griffiths, G.M., 2003. Adaptor protein 3-dependent microtubule-mediated movement of lytic granules to the immunological synapse. Nat. Immunol. 4, 1111–1120.

Forsyth, W.R., Antosiewicz, J.M., Robertson, A.D., 2002. Empirical relationships between protein structure and carboxyl pK_a values in proteins. Proteins 48, 388–403.

Fraser, S.A., Karimi, R., Michalak, M., Hudig, D., 2000. Perforin lytic activity is controlled by calreticulin. J. Immunol. 164, 4150–4155.

Froelich, C.J., Turbov, J., Hanna, W., 1996. Human perforin: rapid enrichment by immobilized metal affinity chromatography (IMAC) for whole cell cytotoxicity assays. Biochem. Biophys. Res. Commun. 229, 44–49.

Grimsley, G.R., Scholtz, J.M., Pace, C.N., 2009. A summary of the measured p*K* values of the ionizable groups in folded proteins. Protein Sci. 18, 247–251.

Hadders, M.A., Beringer, D.X., Gros, P., 2007. Structure of C8alpha-MACPF reveals mechanism of membrane attack in complement immune defense. Science 317, 1552–1554.

Heuck, A.P., Hotze, E.M., Tweten, R.K., Johnson, A.E., 2000. Mechanism of membrane insertion of a multimeric beta-barrel protein: perfringolysin O creates a pore using ordered and coupled conformational changes. Mol. Cell 6, 1233–1242.

Ishiura, S., Matsuda, K., Koizumi, H., Tsukahara, T., Arahata, K., Sugita, H., 1990. Calcium is essential for both the membrane binding and lytic activity of pore-forming protein (perforin) from cytotoxic T-lymphocyte. Mol. Immunol. 27, 803–807.

Kataoka, T., Togashi, K., Takayama, H., Takaku, K., Nagai, K., 1997. Inactivation and proteolytic degradation of perforin within lytic granules upon neutralization of acidic pH. Immunology 91, 493–500.

Kristan, K., Viero, G., Maček, P., Dalla, S.M., Anderluh, G., 2007. The equinatoxin N-terminus is transferred across planar lipid membranes and helps to stabilize the transmembrane pore. FEBS J. 274, 539–550.

Masson, D., Peters, P.J., Geuze, H.J., Borst, J., Tschopp, J., 1990. Interaction of chondroitin sulfate with perforin and granzymes of cytolytic T-cells is dependent on pH. Biochemistry 29, 11229–11235.

McCann, F.E., Vanherberghen, B., Eleme, K., Carlin, L.M., Newsam, R.J., Goulding, D., Davis, D.M., 2003. The size of the synaptic cleft and distinct distributions of filamentous actin, ezrin, CD43, and CD45 at activating and inhibitory human NK cell immune synapses. J. Immunol. 170, 2862–2870.

Metkar, S.S., Wang, B., Aguilar-Santelises, M., Raja, S.M., Uhlin-Hansen, L., Podack, E., Trapani, J.A., Froelich, C.J., 2002. Cytotoxic cell granule-mediated apoptosis: perforin delivers granzyme B-serglycin complexes into target cells without plasma membrane pore formation. Immunity 16, 417–428.

Metkar, S.S., Wang, B., Froelich, C.J., 2005. Detection of functional cell surface perforin by flow cytometry. J. Immunol. Methods 299, 117–127.

Nalefski, E.A., Falke, J.J., 1996. The C2 domain calcium-binding motif: structural and functional diversity. Protein Sci. 5, 2375–2390.

Peterlin, P., Arrigler, V., 2008. Electroformation in a flow chamber with solution exchange as a means of preparation of flaccid giant vesicles. Colloids Surf. B Biointerfaces 64, 77–87.

Peters, P.J., Borst, J., Oorschot, V., Fukuda, M., Krahenbuhl, O., Tschopp, J., Slot, J.W., Geuze, H.J., 1991. Cytotoxic T lymphocyte granules are secretory lysosomes, containing both perforin and granzymes. J. Exp. Med. 173, 1099–1109.

Pipkin, M.E., Lieberman, J., 2007. Delivering the kiss of death: progress on understanding how perforin works. Curr. Opin. Immunol. 19, 301–308.

Ponting, C.P., Parker, P.J., 1996. Extending the C2 domain family: C2s in PKCs delta, epsilon, eta, theta, phospholipases, GAPs, and perforin. Protein Sci. 5, 162–166.

Rizo, J., Sudhof, T.C., 1998. C2-domains, structure and function of a universal Ca^{2+}-binding domain. J. Biol. Chem. 273, 15879–15882.

Rosado, C.J., Buckle, A.M., Law, R.H., Butcher, R.E., Kan, W.T., Bird, C.H., Ung, K., Browne, K.A., Baran, K., Bashtannyk-Puhalovich, T.A., Faux, N.G., Wong, W., Porter, C.J., Pike, R.N., Ellisdon, A.M., Pearce, M.C., Bottomley, S.P., Emsley, J., Smith, A.I., Rossjohn, J., Hartland, E.L., Voskoboinik, I., Trapani, J.A., Bird, P.I., Dunstone, M.A., Whisstock, J.C., 2007. A common fold mediates vertebrate defense and bacterial attack. Science 317, 1548–1551.

Rosado, C.J., Kondos, S., Bull, T.E., Kuiper, M.J., Law, R.H., Buckle, A.M., Voskoboinik, I., Bird, P.I., Trapani, J.A., Whisstock, J.C., Dunstone, M.A., 2008. The MACPF/CDC family of pore-forming toxins. Cell Microbiol. 10, 1765–1774.

Stenger, S., Hanson, D.A., Teitelbaum, R., Dewan, P., Niazi, K.R., Froelich, C.J., Ganz, T., Thoma-Uszynski, S., Melian, A., Bogdan, C., Porcelli, S.A., Bloom, B.R., Krensky, A.M., Modlin, R.L., 1998. An antimicrobial activity of cytolytic T cells mediated by granulysin. Science 282, 121–125.

Stinchcombe, J.C., Bossi, G., Booth, S., Griffiths, G.M., 2001. The immunological synapse of CTL contains a secretory domain and membrane bridges. Immunity 15, 751–761.

Sutton, V.R., Waterhouse, N.J., Baran, K., Browne, K., Voskoboinik, I., Trapani, J.A., 2008. Measuring cell death mediated by cytotoxic lymphocytes or their granule effector molecules. Methods 44, 241–249.

Tschopp, J., Schafer, S., Masson, D., Peitsch, M.C., Heusser, C., 1989. Phosphorylcholine acts as a Ca^{2+}-dependent receptor molecule for lymphocyte perforin. Nature 337, 272–274.

Tweten, R.K., 2005. Cholesterol-dependent cytolysins, a family of versatile pore-forming toxins. Infect. Immun. 73, 6199–6209.

Uellner, R., Zvelebil, M.J., Hopkins, J., Jones, J., MacDougall, L.K., Morgan, B.P., Podack, E., Waterfield, M.D., Griffiths, G.M., 1997. Perforin is activated by a proteolytic cleavage during biosynthesis which reveals a phospholipid-binding C2 domain. EMBO J. 16, 7287–7296.

Voskoboinik, I., Smyth, M.J., Trapani, J.A., 2006. Perforin-mediated target-cell death and immune homeostasis. Nat. Rev. Immunol. 6, 940–952.

Voskoboinik, I., Thia, M.C., Fletcher, J., Ciccone, A., Browne, K., Smyth, M.J., Trapani, J.A., 2005. Calcium-dependent plasma membrane binding and cell lysis by perforin are mediated through its C2 domain: A critical role for aspartate residues 429, 435, 483, and 485 but not 491. J. Biol. Chem. 280, 8426–8434.

Young, J.D., Damiano, A., DiNome, M.A., Leong, L.G., Cohn, Z.A., 1987. Dissociation of membrane binding and lytic activities of the lymphocyte pore-forming protein (perforin). J. Exp. Med. 165, 1371–1382.

Author's personal copy

Zuber, B., Levitsky, V., Jonsson, G., Paulie, S., Samarina, A., Grundstrom, S., Metkar, S., Norell, H., Callender, G.G., Froelich, C., Ahlborg, N., 2005. Detection of human perforin by ELISpot and ELISA: ex vivo identification of virus-specific cells. J. Immunol. Methods 302, 13–25.

Zuber, B., Quigley, M.F., Critchfield, J.W., Shacklett, B.L., Abel, K., Miller, C.J., Morner, A., Paulie, S., Ahlborg, N., Sandberg, J.K., 2006. Detection of macaque perforin expression and release by flow cytometry, immunohistochemistry, ELISA, and ELISpot. J. Immunol. Methods 312, 45–53.